Time dependency of the laser-induced nanostructuring process of chromium layers with different thicknesses on fused silica

P. Lorenz[1], M. Klöppel[2], T.Smausz[3, 4], T. Csizmadia[3], M. Ehrhardt[1], K. Zimmer[1], B. Hopp[3]

[1] Leibniz-Institut für Oberflächenmodifizierung e. V., Permoserstr. 15, D-04318 Leipzig, Germany
[2] Institute of Scientific Computation, Department of Mathematics, TU Dresden, D-01062 Dresden, Germany
[3] Department of Optics and Quantum Electronics, University of Szeged, H-6720 Szeged, Dóm tér 9, Hungary
[4] MTA-SZTE Research Group on Photoacoustic Spectroscopy, University of Szeged, H-6720 Szeged, Dóm tér 9, Hungary

Abstract

Nanostructures exhibit a raised importance in manifold application fields like electronics and optics. The laser irradiation of thin metal layers allows the fabrication of metal nanostructures induced by a melting and deformation process where the resultant structures are dependent on the laser and metal layer parameters. However, for an optimization of this process a detailed physical understanding is necessary. Therefore, the dynamics of the metal layer deformation process was measured by time-dependent reflection and transmission as well as shadow graph measurements at different KrF excimer laser parameters (laser fluence and number of laser pulses) and metal layer thicknesses were used. Magnetron sputtered thin chromium films with a thickness from 10 to 100 nm on fused silica substrates were studied. Based on the optical measurements the liquid phase life time of the metal was estimated and compared with the calculated life time using a simple thermodynamic model.

Keywords: excimer laser, nanostructuring, metal layer, droplet formation, fused silica, chromium

1. Introduction

Nanostructures exhibit a raised commercial interest, e.g. in microelectronic applications. However, the fast and cost-effective production is a big technological challenge where laser methods using self-organization have an outstanding potential.
Different laser methods using self-organization processes of surfaces were developed: 3-dimensional fs laser metal nanostructuring [1-3] and ripple structures formation [5-7] as well as nanostructuring of metal layers [8-12].
This study is focussed on the nanosecond nanostructuring process of thin metal layers. This process is dominated by two physical effects: the laser-solid interaction as well as the mass transport in the liquid. The laser-solid interaction [13-19] can be theoretically described by a heat equation [15, 16] as well as the mass transport in the liquid by a Navier-Stokes equation [10, 20-26]. The consideration of both effects allows a good theoretical description of the laser-induced melting process [11, 27].
A multipulse low laser fluence treatment of the thin metal layer results in the formation of metal droplets [10] where the position of the metal droplets can be controlled by the laser beam profile down to the sub-µm range [28]. The resultant metal droplets dependent on the metal layer thickness is extensively studied [9, 23, 26, 29, 30].
Furthermore, the laser beam scanning procedure [31] as well as the lateral limitation of the metal film [32] influence the nanostructuring process.
However, for the prediction and defined fabrication of nanostructures, in the case of an incomplete metal droplet formation process [26, 27, 29], the knowledge of the time-dependency of the laser-induced liquid metal film is necessary.
Among other things the droplet formation process can be used for the nanostructuring of the substrate surface [11, 12].
In this study, the time-dependency of a KrF excimer laser irradiated thin chromium layer at different layer thicknesses on fused silica was measured by the detection of the time-dependent transmission and reflection signal using a probe cw laser.

2. Experimental details

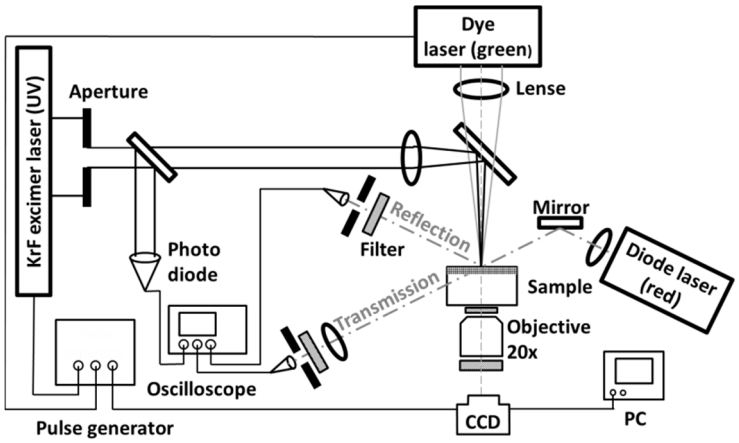

Fig. 1 *Schematic illustration of the experimental set-up.*

The laser-induced modification of a magnetron-sputtered chromium film with different layer thicknesses d = 10 nm, 20 nm, 50 nm, and 100 nm on fused silica was studied, where the chromium film changes was induced by a KrF excimer laser irradiation with a wavelength of $\lambda = 248$ nm and a pulse duration of $\Delta t_p = 25$ ns. The time-dependent behaviour of the melting characteristics of thin metal layers on dielectric substrates was studied with a pump-probe set-up. The used experimental set-up is schematically illustrated in Fig. 1.
Furthermore, the metal layer/fused silica system was irradiated by a red cw diode laser with a wavelength of $\lambda = 660$ nm and a laser power of P = 130 mW, where the transmitted and reflected signal of the diode laser was detected by a photodiode with a time resolution of $\Delta t_{ph} = 1$ ns. The time-dependent signal of the photodiode was recorded by a 1 GHz oscilloscope, where the excimer laser beam was used as reference signal. To reduce the influence of the UV laser radiation onto the measured reflection and transmission signal an aperture/filter combination was used. In Fig. 2 an exemplary transmission and reflection signal is shown. Furthermore, the experimental set-up allows the direct time-dependent optical imaging of the metallic surface structure. Therefore, the Cr/fused silica system was additionally irradiated by an electronically delayed N_2 laser pumped Coumarin 153 green dye laser ($\lambda = 543$ nm, $\Delta t_p = 1$ ns, E = 1 mJ) and the image of the surface structure was displayed by a 20x objective with optical correction of the fused silica thickness into an externally triggered CCD camera. The signal was improved by a band pass filter system for blocking UV and red laser radiation. The time delay $\Delta\tau$ between the KrF excimer laser, the dye laser, and the recording point of the camera could be adjusted by a freely programmable pulse generator. For this study the delay time between both pulsed lasers was fixed at 20 µs.

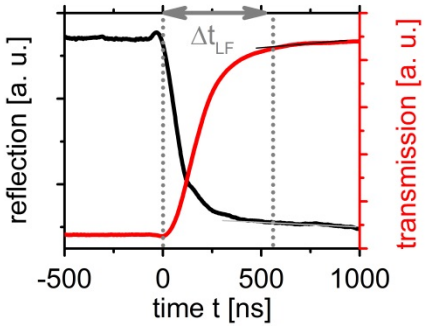

Fig. 2 *Exemplary reflection and transmission signal at 20 nm Cr, N = 1, Φ ~ 930 mJ/cm² (the reflection and transmission signal were smoothed by a low pass filter).*

3. Experimental results

The irradiation of the chromium layer on fused silica with low laser fluences results in a distinct modification of the surface topography induced by a mass transport in the liquid phase [11, 33]. In order to analyse the time behaviour of the deformation process the reflection and transmission signal were detected.
In Fig. 2 the exemplary variation of the reflection and transmission signal of 20 nm Cr on fused silica induced by the irradiation of the sample with approx. 930 mJ/cm² is shown. The irradiation of the 20 nm Cr sample at the first pulse results in a distinct increase of the transmission signal and a decrease of the reflection signal.
The variation of the reflection and transmission signal directly starts at the beginning of the irradiation with the ultraviolet laser pulse at t = 0. Besides the irradiation-induced decrease of the reflection signal, the signal also slightly increased at t ~ 0. This effect can be most likely explained by a minor detection of the UV laser light by the photodiode and, further, an interaction of the electromagnetic field of the KrF excimer laser with the photo diode and the coaxial cable cannot be completely excluded.
The absolute value of the slope of the optical signals decreased at increasing time and finally both signals converged to an almost constant value. The time distance between the beginning of the UV laser pulse and the time position of the convergence is called Δt_{LF} (see Fig. 2). However, the defined and repeatable determination of the convergence point is very difficult due to the signal noise and a low frequency modulation of the signal, e.g. based on a small movement of the sample surface relative to the red laser beam. Therefore the signals were plotted by a linear function (see thin black and grey line in Fig. 2) at a higher time values. The experimentally used convergence point is defined by the point where the signal presented a divergence from the linear plot (see fig. 2).
At $\Phi \sim 930$ mJ/cm², for the irradiation of a thin metal layer d = 20 nm (see Fig. 2), the main variation of the optical signal can be found at the first pulse. For a thicker layer d = 50 nm (see Fig. 3 (b) black square) the distinct variation of the transmission signal can be detected at a higher number of laser pulses.

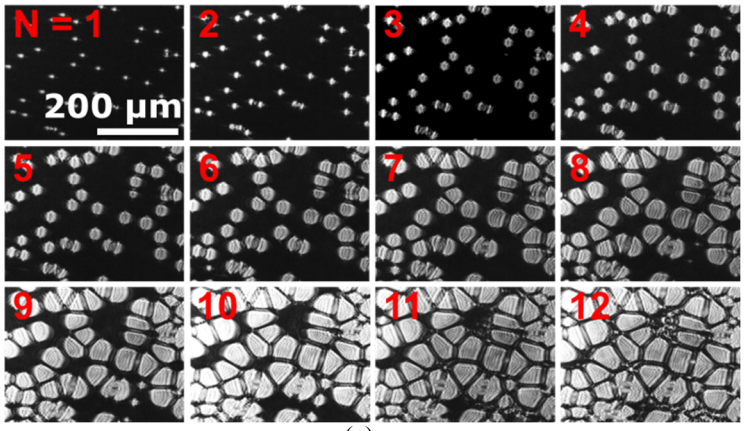

(a) (b)

Fig. 3 *(a) Optical microscopic images: $\Phi = (930 \pm 40)$ mJ/cm², 50 nm Cr on fused silica, $\Delta\tau = 20$ µs.*
(b) Transmission signal and estimated uncovered ratio from the optical images (Fig. 3 (b)) dependent on the number of laser pulses and measured Δt_{LF} at 50 nm Cr and at $\Phi \sim 930$ mJ/cm².

Besides the variation in the optical signal, a distinct modification of the surface morphology induced by the laser irradiation was detected. In Fig. 3 (a) the shadow graph images dependent on the number of laser pulses N for a 50 nm thick chromium film irradiated with ~ 930 mJ/cm² are shown. All images were observed 20 µs after the laser pulse. The irradiation induces the formation of randomly distributed holes in the metal layer. This process starts with the first pulse. The next pulses result in a growth of the existing holes and the formation of new holes. The collision of the holes results in the formation of metal bars. Finally, the multi-pulse irradiation results in the formation of metal droplets. The analysis of the shadow graph images allows the estimation of the uncovered ratio of the fused silica surface. For this, the images were automatically analysed using a photo editing program.
The histogram including a black and white balance was calculated. The resulting brightness distribution shows defined differences between the dark (covered) and bright (uncovered) area which allows the computerized calculation of the uncovered ratio.
The estimated uncovered ratio is summarized in Fig. 3 (b) (red squares). Furthermore, the transmission signal in dependence on the number of laser pulses was measured. The value of the transmission signal after the irradiation is summarized in Fig. 3 (b) (black squares), where the transmission signal was measured at $t >> \Delta t_{LF}$.
The detailed analysis of the transmission signal allows the estimation of the modification time $\Delta t_{LF}(50\text{ nm}, 930\text{ mJ/cm}^2) = (720 \pm 180)$ ns for $N \geq 5$ where the Δt_{LF} is almost independent on the number of laser pulses.

Due to the weak variation of the transmission signal at low number of laser pulses (see Fig. 3 (b) black squares) the Δt_{LF} can only be analysed at higher numbers of laser pulses, in this case for $N \geq 5$. The detected transmission – number of laser pulses behaviour (Fig. 3 (b) black squares) is almost equal to the estimated uncovered ratio (Fig. 3 (b) red squares).
Furthermore, the measurement of the optical signal at different laser fluences Φ and the metal layer thickness Δz allows the estimation of the modification time behaviour $\Delta t_{LF}(\Phi,\Delta z)$. The accuracy of Δt_{LF} is mainly limited by the noise of the measurement signal. Furthermore, for fluences higher than 1 J/cm² the laser irradiation induced a plasma formation process in addition to the melting. Therefore, an influence of the plasma on the optical signal cannot be excluded. However, taking into account plasma measurements in the air the influence time is most likely distinctly smaller than the modification time for thicker metal layers [34, 35].
The modification time for different metal layer thicknesses dependent on the laser fluence is summarized in Fig. 4 where only the transmission signal was used for the estimation of Δt_{LF} due to the better signal-noise ratio at the end of the modification time (see Fig. 2).

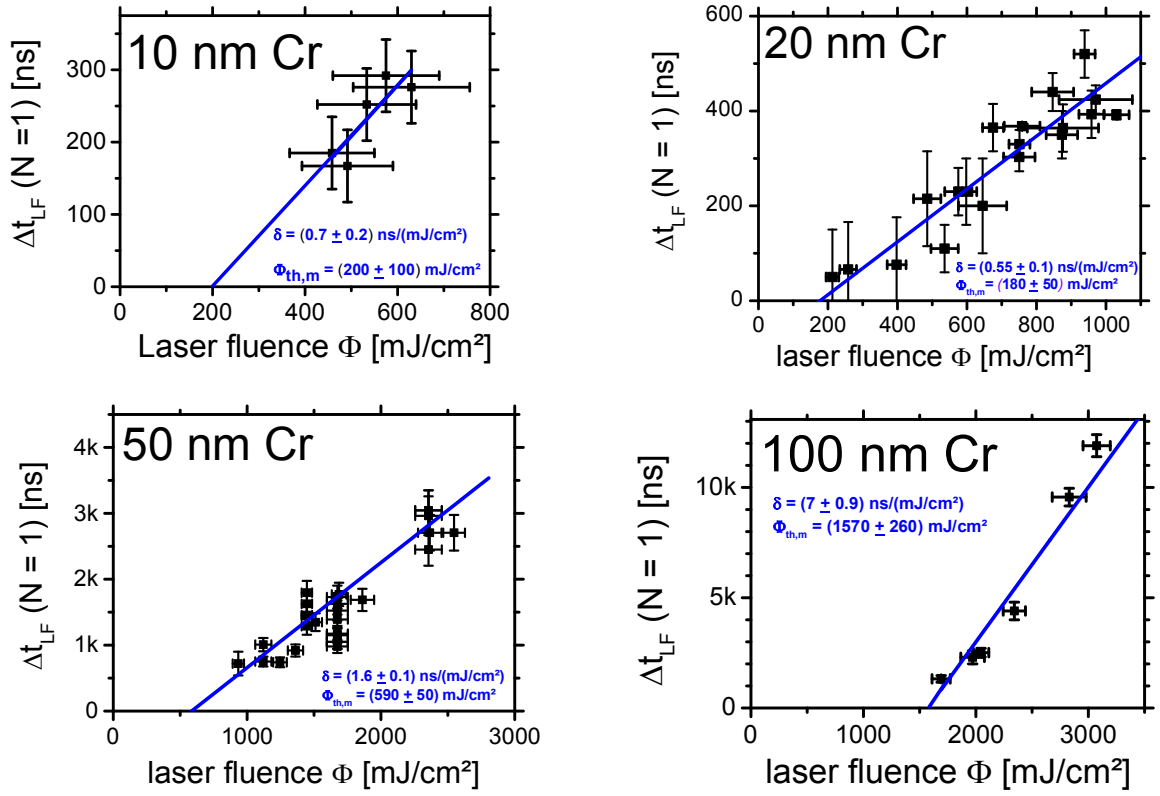

Fig. 4 *Estimated modification time dependent on the laser fluence at different metal layer thicknesses d = 10 nm, 20 nm, 50 nm, 100 nm for the first laser pulse (N = 1) (blue line: linear approximation using Eq. 1).*

The modification time increased for increasing laser fluence and for increasing metal layer thickness.
The Δt_{LF} – laser fluence dependency can be well described by a linear function:

$$\Delta t_{LF}^{N=1}{}_{LF}(\Phi,\Delta z) = \delta(\Delta z)\cdot\left(\Phi - \Phi_{th,m}(\Delta z)\right) \qquad \text{(Eq. 1)}$$

where the fit parameters δ: slope coefficient and $\Phi_{th,m}$: modification threshold are dependent on the metal layer thickness. In Fig. 5 the fit parameter – layer thickness dependency is summarized.

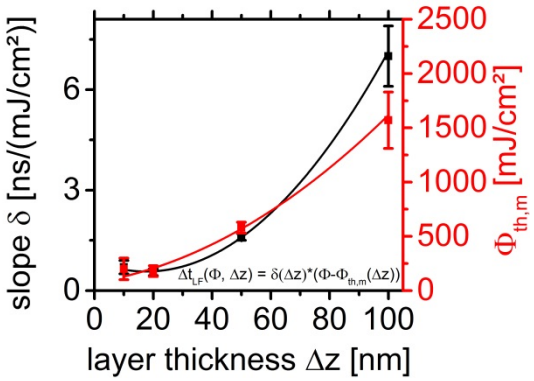

Fig. 5 *Fit parameters δ (black squares) and $\Phi_{th,m}$ (red squares) dependent on the layer thickness using Eq. 1 (see Fig. 4),*
black line: 2nd degree polynomial approximation of the slope – layer thickness dependency using Eq. 2 and
red line: 2nd degree polynomial approximation of the modification threshold – layer thickness dependency using Eq. 3,

$$\delta(\Delta z) \approx \delta_0 + \delta_1 \cdot \Delta z + \delta_2 \cdot \Delta z^2 \qquad \text{(Eq. 2)}$$

with

$\delta_0 = 0.87$ ns/(mJ/cm²) = $8.7 \cdot 10^{-11}$ s³/kg
$\delta_1 = -0.034$ ns/(nm·mJ/cm²) = $-3.4 \cdot 10^{-3}$ s³/(m·kg)
$\delta_2 = 9.68 \cdot 10^{-4}$ ns/(nm²·mJ/cm²) = $9.68 \cdot 10^{4}$ s³/(m²·kg)
with a coefficient of determination of $R^2 = 0.99277$

and

$$\Phi_{th,m}(\Delta z) \approx \beta_0 + \beta_1 \cdot \Delta z + \beta_2 \cdot \Delta z^2 \qquad \text{(Eq. 3)}$$

with

$\beta_0 = 75.1$ mJ/cm² = $7.51 \cdot 10^{2}$ kg/s²
$\beta_1 = 4.35$ mJ/(cm²·nm) = $4.34 \cdot 10^{8}$ kg/(m·s²)
$\beta_2 = 0.11$ mJ/(cm²·nm²) = $1.1 \cdot 10^{18}$ kg/(m²·s²)

with a coefficient of determination of $R^2 = 0.95455$.

In summary, the laser-induced modification time Δt_{LF} of thin chromium is dependent on the laser fluence and the metal layer thickness and can be empirically described by:

$$\Delta t_{LF}^{N=1}(\Phi, \Delta z) = \delta(\Delta z) \cdot \left(\Phi - \Phi_{th,m}(\Delta z)\right) = \left(\sum_{i=0}^{2} \delta_i \cdot \Delta z^i\right) \cdot \left(\Phi - \left(\sum_{k=0}^{2} \beta_k \cdot \Delta z^k\right)\right) \qquad \text{(Eq. 4)}$$

with the fit parameters δ_i and β_k (see Eq. 2 and 3).

4. Theory

Under the assumption that the variation of the optical signal is mainly induced by the modification of the surface topography of the metal layer and that the modification of the surface topography only occurs in the liquid phase, the experimentally identified modification time is almost equal to the laser-induced liquid phase life time. In a first approximation the liquid phase life time can be approximated by solving the heat equation of the laser irradiation – solid interaction:

$$\rho_{Cr,SiO_2} \cdot c_{p;Cr,SiO_2} \cdot \dot{T}(t,\vec{r}_s) - \nabla(\kappa_{Cr,SiO_2} \cdot \nabla T(t,\vec{r}_s)) = Q(t,\vec{r}_s)$$
$$= \begin{cases} \dfrac{\Phi(t,\vec{r}_s)\cdot(1-R_{opt})}{\Delta t_p} \cdot \alpha \cdot \exp(-\alpha \cdot z) & at \quad Cr \\ 0 \quad at \quad SiO_2 \end{cases} \qquad \text{(Eq. 5)}$$

with T: temperature, Q: laser-induced heat source, $r_s = r_s(x, y, z)$: spatial coordinate, ρ: density (Cr: chromium metal layer, SiO_2: fused silica substrate), α: absorption coefficient ($1/\alpha = 10.42$ nm [24]), κ: thermal conductivity, c_p: heat capacity at constant pressure, Φ: laser fluence, R_{opt}: reflectivity (a constant reflectivity of 0.4 was assumed), Δt_p: laser pulse duration. As laser beam profile a top hat beam profile (lateral homogenous laser irradiation) was assumed and the real laser pulse – time dependency was approximated by a 20 ns long rectangular laser beam. Furthermore, the melting and evaporation enthalpies were regarded (see Tab. 1).

	Cr	SiO_2
Melting enthalpy	325 kJ/kg	142 kJ/kg
Evaporation enthalpy	6620 kJ/kg	4340 kJ/kg
Melting temperature T_m	2180 K	1988 K
Evaporation temperature T_{eva}	2755 K	2503 K

***Tab. 1**: Summary of the assumed melting and evaporation enthalpies as well as the temperatures of chromium and fused silica [36, 37].*

The numerical solution of Eq. 5 using a finite element method (FEM) [17] allows the estimation of the temperature distribution. Further information about the assumption in the simulation can be found in Ref. [17]. Based on the calculated temperature distribution, the liquid phase life time Δt_{LF}^{th} can be estimated by using the following definition: Δt_{LF}^{th} is defined by the time range $\Delta t = t_{max} - t_{min}$ on condition $T(x = 0, z = 0, t) \geq T_m^{Cr}$ with $t_{min} \leq t \leq t_{max}$ ($z = 0$: metal layer – fused silica interface). The estimated Δt_{LF}^{th} dependent on the laser fluence Φ at different metal layer thicknesses Δz are summarised in Fig. 6.

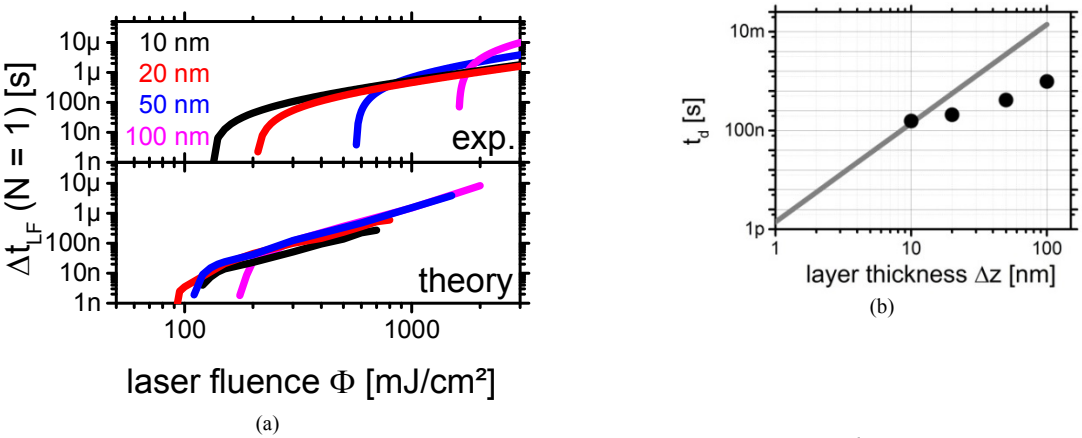

***Fig. 6** (a)Experimentally estimated (using Eq. 4) and theoretically predicted liquid phase life time Δt_{LF}^{th} (using Eq. 5) dependent on the laser fluence Φ at different metal layer thicknesses,*
(b): theoretically calculated dewetting time using Eq. 6(grey) and estimated dewetting time using Eq. 6 (black circle).

Furthermore, based on the theoretical prediction of the droplet and dewetting processes, the droplet formation time and the dewetting time can be estimated dependent on material parameter by Eq. 6, respectively [23].
It is:

$$t_d = \frac{96 \cdot \pi^3 \cdot \gamma \cdot \mu}{A^2} \cdot \Delta z^5 \qquad \text{(Eq. 6)}$$

with μ: viscosity, γ: surface tension, A: Hamaker parameter, and Δz: layer thickness. In Fig. 6 (b) (grey line) the theoretically predicted dewetting time dependent on the layer thickness under the assumption of $\gamma = 0.8$ N/m, $\mu = 1 \cdot 10^{-6}$ kg/(m·s), and $A = 5.7 \cdot 10^{-19}$ J [27] is shown.

5. Discussion

In this study, the dynamics of the laser induced melting deformation of thin chromium layers on fused silica were analysed by shadow graph as well as time-dependent reflection and transmission measurements.
The results show that the laser irradiation of thin chromium layers induces a distinct modification of the surface morphology, where the modification time Δt_{LF} can be estimated from the time-dependent optical signal dependent on the laser parameters as well as on the metal layer thickness. Δt_{LF} increased with increasing laser fluence as well as for metal layer thicknesses $\Delta z \geq 20$ nm increased with increasing layer thickness.
For the experimental values an empiric equation for the interaction of a virgin metal layer with the first pulse could be developed, see Eq. 4.
Under the assumption that the modification of the optical signal, especially of the transmission signal, is mainly defined by the variation of the metal layer topography and that the metal layer modification only occurs in the liquid phase: the experimental determined modification time is almost equal to the liquid phase life time. The laser-induced static variation of the metal layer topography dependent on the laser parameters [9, 23, 26, 29, 30] and especially on chromium layers on fused silica [11, 12, 27, 33] was studied in detail.
Based on the theoretical calculations [23] the necessary droplet formation and dewetting time can be calculated by Eq. 6.
In most cases a multi pulse irradiation of the sample is necessary for the complete dewetting of the metal film (see, e.g. Fig. 2) from the fused silica surface. That means a direct comparison of the experimentally found Δt_{LF} with t_d (see Eq. 6) is not possible. However, in a good approximation the experimental dewetting time t_d^{exp} can be estimated by averaging over all measurement points (M: number of measurement points). t_d^{exp} can be calculated by the summation over all Δt_{LF} up to a maximum number of laser pulses N_{max} where the droplet formation is complete. N_{max} as well as Δt_{LF} is dependent on the laser fluence as well as on the metal layer thickness. It is:

$$t_d^{\exp}(\Delta z) \approx \frac{1}{M} \sum_{l=1}^{M} \sum_{k=1}^{N_{\max}(\Phi_l, \Delta z)} \Delta t_{LF}^{N=k}(\Phi_l, \Delta z) \,. \qquad \text{(Eq. 7)}$$

The resultant t_d^{exp} using Eq. 7 are summarized in Fig. 6 (b) (black circle). For example, for the complete metal droplet formation of a 20 nm thick chromium layer with $\Phi \sim 750$ mJ/cm² two laser pulses are necessary ($N_{max}(\Phi = 750$ mJ/cm², $\Delta z = 20$ nm) = 2). That means, for 20 nm Cr irradiated with $\Phi = 750$ mJ/cm² a t_d^{exp} of ~ 630 ns (see Fig. 3) can be estimated. This is distinctly smaller than the theoretically estimated value of ~ 7.6 μs. With the exception of the 10 nm Cr layer, the approximated dewetting time using Eq. 7 is distinctly lower than the theoretically predicted value (see Fig. 6 (b)). These differences can be explained by a partial evaporation of the chromium during the laser treatment processes, especially at higher metal layer thicknesses, where higher laser fluences were used (see Fig. 3). This results in a reduction of the chromium on the fused silica and, finally, theoretically in a lower dewetting time under the assumption that the chromium reduction can be described by a reduced effective metal layer thickness in Eq. 6.
Furthermore, the liquid phase life time was calculated using a simple thermodynamic model (see Eq. 5). The theory predicted, in agreement with the experimental results, that Δt_{LF} increases with increasing laser fluence. At low metal layer thicknesses ($\Delta z = 10$ nm, 20 nm) a moderate agreement can be found where the simulation predicted a distinct lower threshold at ~ 100 mJ/cm² than the experimental values at ~ 200 mJ/cm² for $\Delta z = 10$ nm and 20 nm. However, for higher metal layer thicknesses there exists a distinct discrepancy between the theoretically and experimentally found values.
The discrepancy between the thermodynamically predicted and experimentally estimated dewetting time can be explained by the theoretical nonobservance of the variation of the surface topography of the metal layer where the hole opening process is non-linear and the opening velocity is not constant, respectively [11]. Furthermore, the mass transport in the liquid-defined material parameters viscosity and surface tension is dependent on the temperature [29, 38]. This suggests that the simple thermodynamic approximation is not sufficient enough to describe the dynamic of the dewetting process. For a successful description a coupling of the liquid-solid interaction, described by Navier- Stokes equation and the laser-solid interaction, described by a heat equation, is necessary.
The comparison of the resultant surface structures of other metal layers [9,10,23,26,39,] with the Cr/fused silica system presents an equal behaviour of the dewetting process. That means, it is expected that other metal/dielectric systems present a similar $\Delta t_{LF}(\Phi)$ behaviour. However, the laser-induced dewetting process is complex dependent on different material parameters like optical absorption coefficient, melting point, surface

tension. Therefore, based on this results a prediction for other metal/dielectric systems is not possible. Further experiments and simulations are necessary to deduce a $\Delta t_{LF}(\Phi)$ for different materials dependent on the material parameters.

6. Conclusions and outlook

The dynamic of the laser-induced melting deformation process of different metal layer thicknesses by measuring the time-dependent reflection and transmission signal was studied.
The analysis of the optical signal allows the estimation of the modification and the liquid phase life time, Δt_{LF} respectively. Furthermore, an empiric equation for Δt_{LF} dependent on the metal layer thickness and on the laser fluence for $N = 1$ can be deduced. In the next step, the extension of the empiric equation for multipulse applications has to be performed.
The experimental value was compared with the simulated liquid phase life time with moderate results. The results suggest that for a successful description of the process a coupling of the Navier-Stokes equation (mass transport in the liquid) with the heat equation (laser-solid interaction) under the assumption of a partial evaporation of the chromium is necessary.
The understanding of the laser-induced dewetting process dependent on the laser parameters (e.g. laser fluence, number of laser pulses as well as laser beam profile) and on the metal layer parameters (e.g. layer thickness) allows the well-defined fabrication of randomly distributed structures. These metal structures can be used as mask structures for a subsequent structuring process or directly for optical applications like low-cost structures with adjustable reflectivity and low-cost infrared resonators.
Furthermore, the application of a periodic modulated laser beam profile allows the fabrication of periodic metal structures in the sub-µm range.

Acknowledgements

We are grateful for funding from the German Research Foundation (DFG: Deutsche Forschungsgemeinschaft) under LO 1986/2-1 and the German Academic Exchange Service (DAAD: Deutscher Akademischer Austauschdienst).

References

[1] A. V. Vorobyev, C. Guo, Optics Express 14 (2006) 2164.
[2] I. N. Zavestovskaya, Quantum Electron. 40 (2010) 942.
[3] A. Pereira, A. Cros, P. Delaporte, S. Georgiou, A. Manousaki, W. Marine, M. Sentis, Appl. Phys. A 79 (2004) 1433.
[4] B. Tan, K. Venkatakrishnan, J. Micromech. Microeng 16 (2006) 1080.
[5] M. Schade1, O. Varlamova, J. Reif, H. Blumtritt, W. Erfurth, H. S. Leipner, Anal. Bioanal. Chem. 396 (2010) 1905.
[6] Y. Yang, J. Yang, L. Xue, Y. Guo, Appl. Phys. Lett. 97 (2010) 141101.
[7] R. LeHarzic, Optics Express 13 (2005) 6651.
[8] S. Imamova, A. Dikovska, N. Nedyalkov, P. Atanasov, M. Sawczak, R. Jendrzejewski, G. Śliwiński, M. Obara, J. Optoelectron. Adv. Mater. 12 (2010) 500.
[9] S. J. Henley, C. H. P. Poa, A. A. D. T. Adikaari, C. E. Giusca, J. D. Carey, S. R. P. Silva, Appl. Phys. Lett. 84 (2004) 4035.
[10] K. Ratautas, M. Gedvilas, G. Račiukaitis, A. Grigonis, J. Appl. Phys. 112 (2012) 013108.
[11] P. Lorenz, M. Klöppel, F. Frost, M. Ehrhardt, K. Zimmer, P. Li, Appl. Surf. Sci. 280 (2013) 933.
[12] P. Lorenz et al., Appl. Phys. A 111 (2013) 1025-1030.
[13] E. Matthias, M. Reichling, J. Siegel, O. W. Käding, S. Petzoldt, H. Skurk, P. Bizenberger, E. Neske, Appl. Phys. A 58 (1994) 129.
[14] S. J. Henley, J. D. Carey, S. R. P. Silva, Phys. Rev. B 72 (2005) 195408.
[15] D. Bäuerle, Laser Processing and Chemistry, 3rd Ed., Springer, Berlin, Heidelberg, New York, 2000.
[16] R. F. Wood, G. E. Giles, Phys. Rev. B 23 (1981) 2923.
[17] P. Lorenz, M. Ehrhardt, K. Zimmer, Appl. Surf. Sci. 258 (2012) 9138.
[18] P. Lorenz, M. Ehrhardt, K. Zimmer, Appl. Surf. Sci. 258 (2012) 9742.
[19] P. Lorenz, M. Ehrhardt, K. Zimmer, Proc. SPIE 8243 (2012) 82430Y.
[20] A. Sharma, R. Khanna, Phys. Rev. Lett. 81 (1998) 3463.
[21] A. Yochelis, E. Knobloch, L. M. Pismen, Eur. Phys. J. E 22 (2007) 41.
[22] A. Vrij, Discuss. Faraday Soc. 42 (1966) 23.
[23] Ch. Favazza, R. Kalyanaraman, R. Sureshkumar, Nanotechnology 17 (2006) 4229.
[24] S. J. Henley, J. D. Carey, S. R. P. Silva, Appl. Surf. Sci. 253 (2007) 8080.
[25] D. A. Willis, X. Xu, J. Heat Transfer 122 (2000) 763.
[26] J. Trice, D. Thomas, Ch. Favazza, R. Sureshkumar, R. Kalyanaraman, Phys. Rev. B 75 (2007) 235439.
[27] P. Lorenz, M. Klöppel, T. Smausz, T. Csizmadia, M. Ehrhardt, K. Zimmer, B. Hopp, "Dynamics of the laser-induced nanostructuring of thin metal layers: Experiment and theory" Materials Research Express submitted.
[28] M. Mäder, T. Höche, J.W. Gerlach, R. Böhme, B. Rauschenbach, Physical Status Solidi B 247 (2010) 1372.
[29] George Kaptay, "A unified equation for the viscosity of pure liquid metals", Z. Metallkd. 96 (2005) 1.
[30] K. Ratautas et al., JLMN 7 (2012) 355.
[31] M. GEDVILAS, G. RAČIUKAITIS, K. REGELSKIS, P. GEČYS, Journal of Laser Micro/Nanoengineering 3 (2008) 58
[32] Y. Wu, J. D. Fowlkes, N. A. Roberts, J. A. Diez, L. Kondic, A.G. Gonzalez, P.D. Rack, Langmuir 27 (2011) 13314
[33] P. Lorenz et al., NSTI - Nanotech 1 (2013) 686.

[34] Zeng, Xianzhong J.; Mao, Xianglei; Greif, Ralph; Russo, Richard E, High-Power Laser Ablation V. Edited by Phipps, Claude R. Proceedings of the SPIE, Volume 5448, pp. 1150-1158 (2004).
[35] Xiangtai Wang and Baoyuan Man, Journal of the Korean Physical Society, Vol. 32, No. 3, March 1998, pp. 373 – 379.
[36] http://www.mt-berlin.com/frames_cryst/descriptions/quartz%20.html, March 2014.
[37] W.M. Haynes (Ed.), Handbook of Chemistry and Physics, 93rd edition, CRC Press, Taylor & Francis Group, Boca Raton, London, New York, 2012.
[38] Takamichi et al: The physical properties of liquid metals, Oxford Calderon Press (1993).
[39] H. Krishna, N. Shirato, S. Yadavali, R. Sachan, J. Strader, R. Kalyanaraman, ACSNANO 5 (2011) 470